




Virtual Hippotherapy for the Treatment of Idiopathic Scoliosis

D. Rösner¹ , G. Brunnett¹ , S. Israel², G. Kaden³, M. Kehr⁴, T. Kronfeld¹ 

¹TU Chemnitz, Germany

²sanisax GmbH, Dresden, Germany

³SATRON GmbH, Zschopau, Germany

⁴Kehr Sport GmbH, Zschopau, Germany

Abstract

We present a prototype of an integrated virtual reality (VR) system which is intended to supplement traditional therapeutic practices for the conservative treatment of idiopathic scoliosis. Our solution is inspired by equine-assisted therapy (hippotherapy) and includes a horse riding simulator, therapist GUI as well as a synchronized visualization using either a conventional monitor or a head-mounted display (HMD) as an output device. A proof-of-concept study indicates that the system could constitute a valuable addition to the practice of physical therapy.

CCS Concepts

• **Applied computing** → **Consumer health**; • **Computing methodologies** → **Virtual reality**; • **Human-centered computing** → **Virtual reality**;

1. Introduction

Virtual reality has evolved tremendously over the past thirty years and developments in the field are still occurring at an astonishing rate. Rather than focusing purely on the visual output, many modern systems seek to offer an integrated multisensory experience geared towards full sensory immersion. Besides the inclusion of sound and specialized input devices, haptic feedback constitutes an important prerequisite for achieving that goal in many applications [AGHWK16].

Following a recent wave of affordable consumer hardware, virtual reality has found a number of use cases in the realm of physical therapy [WKL14]. Naturally, such systems could benefit greatly from incorporating haptic stimuli. To that end, we developed a prototype of a VR-based therapy machine for the *conservative* (non-surgical) treatment of *idiopathic scoliosis*. Beyond that, the proposed approach could be adapted for other musculoskeletal disorders or for usage in general entertainment. As part of this paper, we submit the following contributions:

Mechatronic Therapy Device The development of the presented system is motivated by the practice of *hippotherapy* which aims to supplement traditional physiotherapy with horseback riding in order to increase the patient's strength, control and posture [AKB*15]. Consequently, we constructed a therapy machine that mimics the physical experience of riding on a horse. It also dynamically applies lateral forces to the patient's torso, encouraging them to actively develop their musculature in a way that alleviates their scoliosis.

Therapist GUI The graphical user interface enables the therapist to manage therapy sessions and facilitates control over the operation of the machine. Its core feature is an editor which can be used to specify the forces that are applied by the therapy machine as functions of time.

Virtual Environment Physical stimulation is complemented with visual feedback which provides the impression of sitting on a horse and riding through a landscape. The virtual environment can either be viewed monoscopically on a traditional monitor or through a consumer-grade HMD to increase the effect of immersion. To provide a consistent experience of physical and visual stimuli, different mechanisms ensure that the visualization and the forces generated by the therapy machine remain properly synchronized. This includes the alignment of the virtual horse's gait with the motion of the physical saddle as well as a correction algorithm which ensures a consistent camera position. Furthermore, the *net force* applied to the patient's torso is at any point in time proportional to the curvature of the path that the horse is following, allowing the patient to associate the lateral forces generated by the machine with the movement inside the virtual environment.

User Study To evaluate the general design and functionality of the therapy system we conducted a qualitative study with patients suffering from idiopathic scoliosis. Judging from this initial experiment, the VR-based therapy system seems to provide an engaging user experience. Furthermore, the increased sensory immersion from wearing a head-mounted display was preferred by most participants. Based on the results of this study we conclude that, with

some improvements, the presented VR system has the potential to be applied by therapists in their daily work. Thus, our prototype opens the possibility to examine the medical efficacy of virtual hippotherapy for the treatment of idiopathic scoliosis in quantitative studies.

The remainder of this paper is structured as follows: We begin by giving an overview of related research in section 2. Following that, section 3 contains a description of the three system components (mechatronic device, graphical user interface and visualization). Finally, we evaluate the results of our work in section 4.

2. Related Work

According to the German Robert Koch Institute (RKI), 5.2% of adolescents under the age of 18 exhibit an unexplained side-to-side curvature of the spine of more than 10° and are therefore diagnosed with *idiopathic scoliosis* [KAE*07]. The term *idiopathic* refers to the fact that the cause of the deformity is unknown and stands in contrast to *non-idiopathic scoliosis*, which can be traced back to malformed vertebrae, neuromuscular insufficiencies such as cerebral palsy or a lack of passive stabilizers of the spine [KSK13]. As a well-established conservative treatment for idiopathic scoliosis, Schroth therapy [LS92] combines a special breathing technique with active muscle training to alleviate spine deformities. Much of the therapeutic background for the proposed machine is rooted in this approach. Wibmer et. al. [WGN*16] integrate a video game that provides physical exercise with the Schroth method, reporting increased motivation and exercise performance. In their system, a game controller is used to track two points on the patient's body while the output is displayed on a conventional monitor.

Equine-assisted therapy or *hippotherapy* has been applied to the treatment of several musculoskeletal disorders including cerebral palsy [BMG03,MBDSS09], low back pain [JGS*15,AML*16] and multiple sclerosis [HNF*05]. In their 2015 review, Angoules et. al. report improvements in muscle strength, balance, coordination, relaxation and posture control [AKB*15]. However, the cost and effort required to keep a real horse severely limit the availability of horse riding in general and hippotherapy in particular. As a result, several horse riding simulators have been developed [BK13] and used for therapeutic purposes [HKK*12,RLZ21]. For example, Anderson et. al. [AABB10] reproduce prerecorded horse motion data on a hexapod robotic platform and enable the user to explore a predefined virtual environment through a multisensory VR system. The authors also include various sensors to facilitate quantitative studies regarding the effects of equine-assisted therapy. However, we found no indication that this system has ever been used for such a study. In contrast to their work, we utilize a moving platform with fewer degrees of freedom while synchronizing the visual output with the motion of the simulator. Additionally, we induce haptic stimuli by applying lateral forces to the user's torso. Furthermore, our virtual environment is generated procedurally, providing the therapist with greater control over the setting. Kim et. al. [KNS19] reported promising results using VR in combination with a 5-DOF horse riding simulator to improve functional performance in children with cerebral palsy. A 9-axis inertial measurement unit (IMU) was affixed to the simulator and used to synchronize the virtual environment to the movements of the machine via bluetooth. Un-

fortunately, the paper provides no information regarding the content of the virtual environment and the exact synchronization algorithm. The setup of the electromechanical device which simulates riding motions differs in two ways: First, our machine tracks the saddle position directly instead of relying on an external sensor. This eliminates the IMU as an error source and reduces the transmission latency by utilizing Ethernet or Wi-Fi instead of Bluetooth. However, in the interest of cutting the cost of production and maintenance, our design features only one degree of freedom. Second, their system applies no external forces to the torso of the patient, relying on a therapist to continuously correct the patient's upper body posture. In our solution, mechanics, user control and visualization are fully integrated.

On a broader spectrum, virtual reality has been used to treat a number of disorders [WW05,GTC*15,YÇD*17] and to supplement traditional physiotherapy following brain and limb injuries [LMM12,PCSB*18]. For a comprehensive overview of VR in the context of motor rehabilitation, see also [WKL14]. Concerning the role of the therapist in relation to virtual reality, Levac and Galvin [LG13] suggest that personal interaction with the patient remains crucial in the application of VR-based therapy.

In an effort to convey more than just visual stimuli, many modern consumer-grade HMDs feature integrated headphones. Furthermore, specialized hardware for the conveyance of smell [MNI11] and taste [KJH*18] as well as a plethora of innovative input devices have been developed [AGHWK16]. Systems that rely on omnidirectional treadmills or low-friction surfaces for navigating virtual worlds usually outfit the user with a harness that guarantees stability without an active mechanical element [NB16]. A similar concept has been leveraged by Fels et. al. to simulate swimming [FKC*05]. In their installation, the user is suspended horizontally in mid-air and experiences buoyancy and drag forces through a combination of bungee cords, pulleys and counterweights. Haptic feedback vests serve as an additional output channel and have been used to actively convey vibrations, sound, electrical stimuli and temperature changes [LPYS04,AGHWK16]. Our system combines features of the above approaches, with the vest itself constituting a passive element and forces being applied by means of external motors connected via ropes. In the current prototype, these forces serve a purely therapeutic purpose. However, a similar method could be used to mimic centripetal forces, e.g. in motorcycling simulators.

3. System

The proposed system encompasses a mechatronic horse riding simulator, a therapist GUI and a synchronized visualization. Figure 1 illustrates their relationship.

3.1. Mechatronic Device

The mechatronic device as seen in figure 2 consists of several components. An ergonomic stool which resembles a saddle is affixed to a raised platform. Aside from being height-adjustable, the two sides of the seat can also be tilted forwards and backwards independently, allowing therapists to adjust the setup according to the patient's default hip posture. While sitting on the saddle, a static handlebar offers support as needed. An electric motor drives the

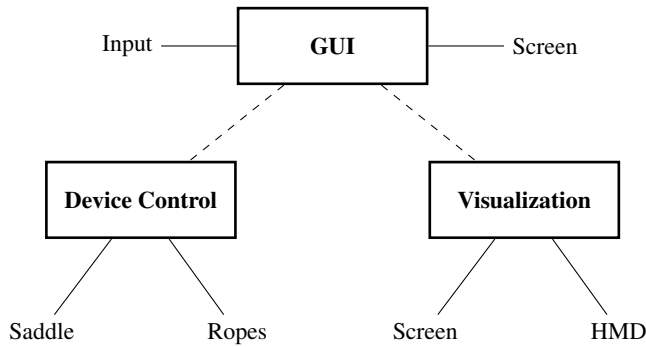


Figure 1: A schematic overview of the therapy system. Solid lines represent connections to peripheral devices while dashed lines constitute network connections.

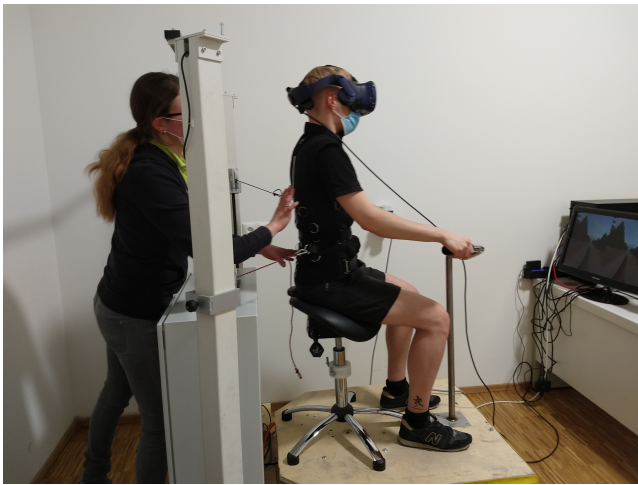


Figure 2: The therapy machine in use during a test run. The therapist is monitoring the patient's posture while also keeping an eye on the GUI on a screen to the right. Both ropes have been attached at specific points on the vest and their pulleys adjusted vertically according to the type of scoliosis at hand.

platform itself, offering one DOF by tilting the plane forwards or backwards. We refer to one *cycle* as the time it takes the saddle to, starting from a neutral position, move forward to its limit, then backward to its limit and then forward to the neutral position. Each cycle ends with a *synchronization event*. The number of cycles per second is referred to as the saddle's *frequency*. In case of emergency, a button next to the patient's left foot can be used to stop the machine immediately.

Behind the saddle, two pillars are attached to the machine's base. At the bottom of each of them, an electric winch pulls on a rope which runs up inside the pillar and across a height-adjustable pulley. Both ropes end in a spring hook. By attaching these hooks to different rings on a custom vest and changing the height of the pulleys, therapists can apply force at various points on the patient's torso, depending on the type of scoliosis they exhibit. The pillars can be detached from the base and transported separately which re-

duces the width of the entire device to below 80 cm, allowing it to fit through most standard doorways.

Inside the cabinet at the back of the machine, a number of electronic components control the speed of the saddle motor as well as the force applied to each of the ropes. A network interface accepts commands to change these parameters via Ethernet and sends status updates, such as the current saddle angle and the actual forces applied by the ropes, back to the rest of the system.

3.2. GUI

The GUI application constitutes the primary means of interaction between the therapist and the system. It has been developed using the Unity engine to facilitate portability to a wide variety of platforms. When launched, it establishes a network connection with the mechatronic device and presents a list of all patients that have been entered into the internal database. New patients can be added through an input mask and patient-specific data can be accessed by clicking on an entry in the list. This data includes personal information, comments by the therapist and a list of therapy sessions performed with the patient. Selecting a session displays the session detail screen. There, the therapist is able to enter session-specific comments and to access a dedicated editor for planning the forces applied to the ropes described in section 3.1 over the course of the session. The force progression is described as a vector valued function

$$F(t) = (F_L(t), F_R(t)) \quad (1)$$

where the component functions F_L and F_R are associated with the forces applied to the left and right rope respectively when viewed from behind the patient. Each of these functions is defined via a sequence of $n \in \mathbb{N}$ *keypoints*

$$k_0 = (0, f_{min}) \quad (2)$$

$$k_i = (t_i, f_i) \quad i = 1, \dots, n-1 \quad (3)$$

with f_i determining the force to be applied to the respective rope t_i seconds after the beginning of the therapy session. f_{min} and f_{max} denote the minimum and maximum force that can be generated by the electric winch, i.e. $0 < f_{min} \leq f_i \leq f_{max}$. These parameters are retrieved over the network during the initialization of the GUI. Between two keypoints, the resulting force is obtained through linear interpolation. Beyond the final keypoint, the force remains constant.

The editor shown in figure 3 displays the graphs of F_L and F_R with the elapsed time and the applied force along the horizontal and vertical axis, respectively. Individual keypoints can be added, modified and removed. Since it is a common use-case to match the forces to the patient's breathing rhythm, a wizard allows therapists to easily produce regular patterns like the one shown in the image. Finally, the current function can be saved and reused at a later date.

Once the force progression is prepared and the patient is seated on the saddle, the therapy session can be started from within the

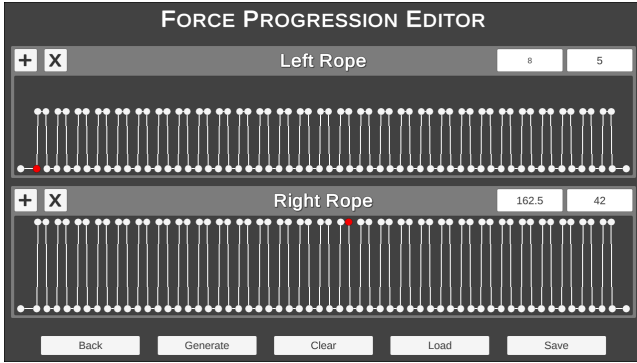


Figure 3: The force progression editor with the force function for the left rope on top. Individual keypoints can be added and removed using the buttons on top and modified by dragging and dropping or by entering specific values into the input fields. The currently selected keypoint is highlighted in red.

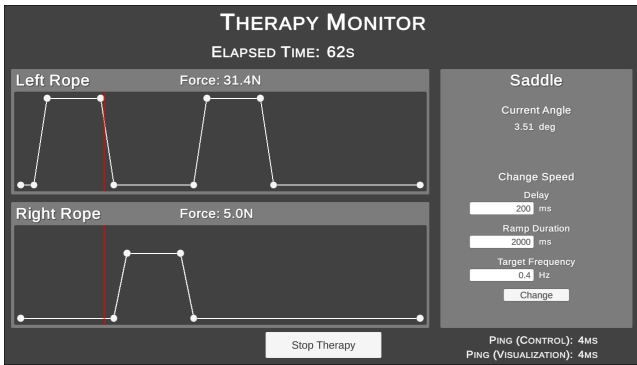


Figure 4: The therapy monitor with information about the current force progression on the left and saddle frequency controls on the right. The red line marks the current point in time along the force progression.

session detail screen of the GUI. While it is running, the force progression and current saddle angle can be monitored on screen as shown in figure 4. Furthermore, the speed of the saddle can be changed at will by entering the desired frequency, the delay until the adjustment begins and the duration over which it should occur.

3.3. Visualization

Initiating a therapy session will also start the visualization software which immediately accepts a network connection from the GUI. This architecture allows for the two applications to run on separate machines, for example a desktop PC for the visualization and a tablet for the GUI. The software and the underlying custom engine were developed in C++ using the OpenVR SDK to interface with the head-mounted display.

Environment Upon launch, the current force progression is transmitted to the visualization and converted into a path across a 3D terrain which is subsequently followed by the virtual horse. This

process is based on the concept of *net force*, the difference between the force applied to the left and right rope at any given time:

$$F_N(t) = F_L(t) - F_R(t) \quad (4)$$

Whenever the net force is positive, the pull on the left rope is stronger and the path will be curved to the left. Conversely, a negative net force indicates a stronger pull on the right side and a bend to the right. If the net force is zero, the path should lead straight on. In other words, F_N is proportional to the curvature of the path in the 2D plane viewed from above. This lets the path serve as a visual aid to the patient, indicating force changes ahead of time. The conversion is achieved by means of the following steps:

1. We sample the net force with a configurable step size s denoting the time between two samples in seconds. The default value $s = 0.1$ produces a sufficiently fine-grained sampling so that the effects of interpolating between samples (see below) are not noticeable.
2. Each net force sample is multiplied with a scalar r to obtain curvature values κ_i . This parameter intuitively determines how tightly the path bends for any given net force value and can be set by the therapist based on the requirements of the patient.
3. Position, tangent and normal samples (\mathbf{p}_i , \mathbf{t}_i and \mathbf{n}_i , respectively) of a 2D curve are computed using the curvature samples as well as an initial position \mathbf{p}_0 and tangent \mathbf{t}_0 :

$$\mathbf{p}_i = \mathbf{p}_{i-1} + s\mathbf{t}_{i-1} \quad (5)$$

$$\mathbf{t}_i = \frac{\mathbf{t}_{i-1} + s\kappa_{i-1}\mathbf{n}_{i-1}}{\|\mathbf{t}_{i-1} + s\kappa_{i-1}\mathbf{n}_{i-1}\|} = (x_{ii}, y_{ii})^T \quad (6)$$

$$\mathbf{n}_i = (y_{ii}, -x_{ii})^T \quad (7)$$

4. We procedurally generate a terrain heightmap using Perlin noise [Per85, Per02, Gre05]. To increase the frequency range of the output, several *octaves* of noise at different amplitudes and frequencies are added together. This technique is known as *fractal noise* [EMP*03]. The height value of a point \mathbf{p} in the XZ-plane is therefore calculated as

$$h(\mathbf{p}) = \sum_{i=0}^{n-1} a\alpha^i f(b\beta^i \mathbf{p}) \quad (8)$$

where n is the number of octaves, f is the noise function, a is the base amplitude and b is the base frequency of the noise. *Persistence* (α) and *lacunarity* (β) control the amplitude and frequency at higher octaves. These parameters can be tweaked to produce a wide variety of surface structures, from flat plains over rolling hills to jagged mountains. In the current prototype, they are chosen in a way that avoids steep slopes which would be difficult for a horse to traverse ($a = 25$, $b = 2$, $\alpha = 0.5$ and $\beta = 2$). A more sophisticated solution which incorporates the constraints that are implied by the 2D path directly into the terrain generation is currently under development. The position and size of the terrain are determined by the bounding box of the 2D curve so that each point on the path is at least a certain, user-defined distance away from the edge of the terrain.

5. Since the generated surface is continuous by definition, tangents and normals for the terrain vertices can be calculated using finite differences. Let δ be the edge length of a cell in the heightmap. Given the height values h_l , h_r , h_t and h_b of the four adjacent vertices (see figure 5), two axis-aligned tangents \mathbf{t}_x and \mathbf{t}_z as well as the normal vector \mathbf{n} of a terrain vertex \mathbf{v} can be calculated as follows:

$$\mathbf{t}_x = \frac{(2\delta, h_r - h_l, 0)^T}{\|(2\delta, h_r - h_l, 0)^T\|} \quad (9)$$

$$\mathbf{t}_z = \frac{(0, h_b - h_t, 2\delta)^T}{\|(0, h_b - h_t, 2\delta)^T\|} \quad (10)$$

$$\mathbf{n} = \frac{\mathbf{t}_z \times \mathbf{t}_x}{\|\mathbf{t}_z \times \mathbf{t}_x\|} \quad (11)$$

Whenever an adjacent height value is unavailable, i.e. along the edges of the terrain, forward or backward differences are employed as needed. Height values between vertices can be obtained via bilinear interpolation. Since normals and tangents are unit vectors representing points on a sphere, they are interpolated spherically instead [Sho85].

6. Decorative objects are placed pseudorandomly so that they don't overlap each other or the path.
7. We combine position samples from the 2D curve with terrain height values to obtain 3D curve position samples. Tangent and normal samples for this curve are taken directly from the terrain.

These 3D curve samples are used to set the position and orientation of the virtual horse according to the time that has elapsed since the beginning of the therapy session. Position values between two sample points are obtained using linear interpolation. As before, SLERP is used for normals and tangents. Figure 6 shows an example of an environment created using this algorithm.

Animation The motions of the virtual horse are produced using forward kinematics. An animation clip of a walking horse has been manually adjusted so that the start of the clip matches the neutral position of the saddle and one iteration of the clip corresponds to one full cycle. During runtime, the simulation receives frequency changes and synchronization events over the network and corrects

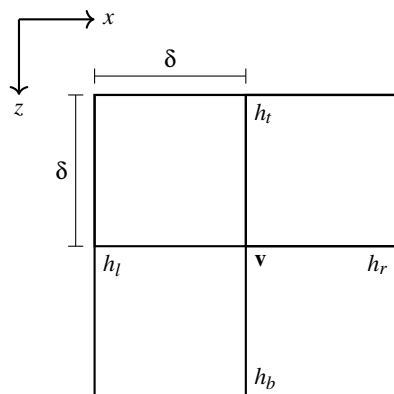


Figure 5: The four height values used to calculate tangents along the X- and Z-axis at the terrain vertex \mathbf{v} .

the associated timestamps for latency. The speed of the animation is then set according to the current frequency. Whenever a synchronization event is recorded, the animation clip is reset to its beginning. Since frequency changes are not instantaneous and mechanical errors accumulate gradually, this proved sufficient to prevent desynchronization without noticeable visual artifacts.

For therapeutic reasons, the therapist must be able to change the frequency of the saddle at will during runtime. Recall however, that the parameter of the force progression $F(t)$ represents the time since the beginning of the therapy session. Therefore, the horse's path and the speed at which it moves forward remain constant for the duration of a session. This can produce unrealistic output since it effectively disconnects the animation from the horse's movement across the terrain. Consider the case when the therapist decides to stop the saddle because a patient reports discomfort, but wishes to continue the therapy session. As long as the saddle remains static, the virtual horse would then loop through its "idle" animation while still moving forward normally, seemingly gliding across the terrain. However, based on our tests we surmise that such a scenario constitutes a rare edge case. One possible solution to this problem would be a separate "free roam" mode in which the movement of the virtual horse is not tied to the total elapsed time.

A more sophisticated animation module might utilize inverse kinematics (IK) to prevent the horse's limbs from clipping through the terrain. However, since it is quite hard for the user to even look at the hooves from a first person perspective, IK was not incorporated into this system. Furthermore, the current curvature of the path could be used to blend between three animation clips for walking left, right and straight ahead. In our prototype, this was not included because we assume the maximum curvature of the path to be relatively small for therapeutic reasons.

Output Our system features two visual output modes: monoscopic display on a conventional monitor – hereafter referred to as *screen mode* – or virtual reality using a HMD. This option is provided both as a means to gauge the impact of VR compared to traditional 2D output and as a way to alleviate stress for patients that feel uncomfortable in a VR environment. Both modes place the user in a first-person viewpoint on horseback. In screen mode, the camera always looks straight ahead whereas users are able to turn it freely by moving their head in VR mode. The origin of the tracking coordinate space is calibrated to lie on top of the saddle.

Due to the construction of the mechatronic device simulating the horse ride, the saddle pivots around the base of the platform shown in figure 2, causing the user to continuously move forwards and backwards in real space. If the tracked head position is applied directly to the virtual camera, the viewpoint would slide back and forth even when sitting perfectly still. During development, this was perceived as highly unrealistic. Therefore, we implemented an algorithm to eliminate the effects of the saddle motion from the camera transformation while preserving the user's head movement relative to the saddle. To that end, two parameters are utilized in addition to the tracking data provided by the HMD:

1. The distance between the pivot point and the top of the saddle which is measured manually and stays fixed over the duration of a therapy session.

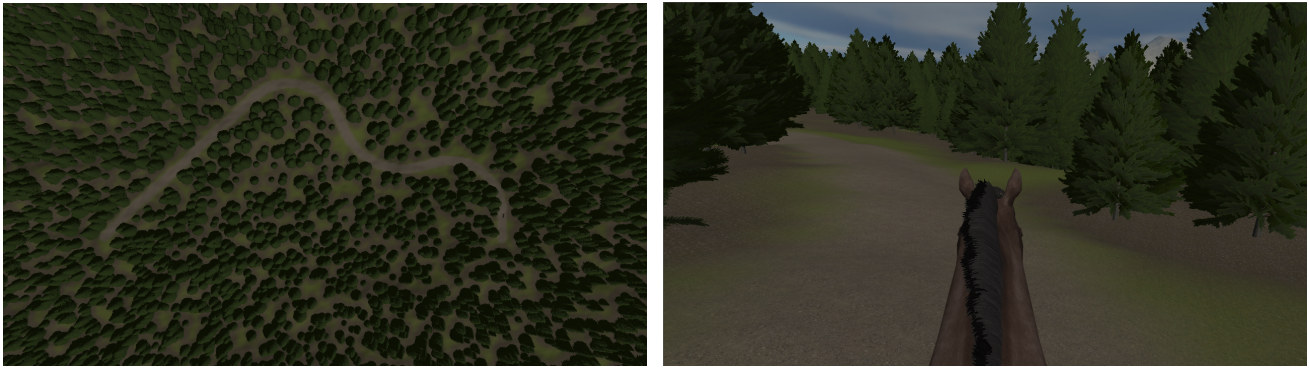


Figure 6: Left: The path generated from the force progression in figure 4. It starts on the right side of the picture, exhibiting two bends to the left, one to the right and a straight stretch towards the end. Right: First-person view from horseback in screen mode.

2. The current angle of the saddle which is recorded and transmitted by the therapy machine at regular intervals (10 Hz by default).

After being corrected for network latency, the angle is linearly extrapolated into the present and used to calculate the difference between the saddle's neutral and current position. The resulting offset is added to the tracked head position, producing a stable virtual camera. Once again, changes in the observed parameter are small and gradual, causing no noticeable jittering under this simple algorithm.

4. Evaluation

The three aforementioned components have been successfully combined into a functional integrated VR solution. This section provides an evaluation of the system's performance and usability.

4.1. Performance

A PC equipped with an AMD Ryzen 7 3700X CPU and an NVIDIA GeForce RTX 2070 SUPER graphics card is able to run the visualization consistently at 90 frames per second which is equivalent to the refresh rate of the HMD that was used for the prototype (HTC Vive Pro). On the same machine, the preprocessing steps detailed in section 3.3 are completed in less than five seconds.

Figure 7 shows a measurement of the current saddle angle across time. This variable is recorded by the machine control and sent across the network to the visualization every 100 ms. Since it forms the basis for the camera correction described in section 3.3, which is a likely candidate for causing simulation sickness, its synchronicity should be examined. The data reveals a deviation of about 0.25° at the extrema and no appreciable temporal offset. Readings were obtained with the machine control connected via Ethernet to a PC running both GUI and visualization.

4.2. User Study

In order to assess the usability of our system for the therapy of patients with scoliosis we conducted a qualitative user study in cooperation with a physiotherapist who is familiar with Schroth therapy.

Technical Setup The study was performed in a lab provided by sanisax GmbH in Dresden, Germany. In preparation of the experiment, the mechatronic device was positioned so that it would be accessible from the front and back as well as from one of the sides. The default saddle frequency was set to 0.4 Hz, i.e. one cycle every 2.5 seconds. Two monitors (both 24 inches, 1080p, 60 Hz) were placed on a table roughly one meter in front of the device. One of them was used to display the visualization while the other one showed the therapist GUI. A mouse and keyboard were provided to enable interaction with the user interface. Both the GUI and the visualization ran on the same PC that was used to obtain the performance measurements presented in section 4.1. The connection between the mechatronic device and the PC was established via Ethernet. Two SteamVR Base Stations 2.0 were affixed in the room with a clear line of sight to the saddle and an HTC Vive Pro served as the HMD for the experiment. In the interest of hygiene, the foam padding inside the HMD was replaced with a wipeable variant.

Participants Patients who suffered from idiopathic scoliosis were eligible for inclusion in the study. Individuals with non-idiopathic scoliosis were excluded. Gender was not restricted. Consequently, nine patients aged 13 to 32 (mean: 23.8, SD: 7.1) were invited to participate.

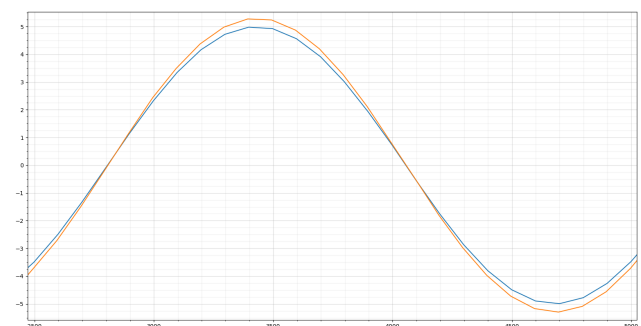


Figure 7: The current saddle angle in degrees as logged by the machine control (blue) and the visualization (orange). Time is given in milliseconds along the horizontal axis.

Procedure Before the start of the first experiment, the therapist was instructed in the operation of the prototype. This included a personal test run in order to gain an intuitive understanding of the forces which can be applied by the machine.

Each participant completed a set of four consecutive five-minute therapy sessions with a short break of one to two minutes between them. For the first two sessions of each set, the visualization operated in screen mode while sessions three and four were performed using the HMD. Before the start of a set, the therapist customized the force progression and the attachment pattern of the ropes according to the type of scoliosis at hand. To that end, each patient was asked to take several deep breaths. A force progression was then generated based on the duration of these breaths so that during each inhalation, both ropes would pull with a force proportional to the magnitude of the spinal curve to which they are attached. The exact force values were determined subjectively by the therapist. To illustrate, consider the force progression in figure 3 which was prepared for a patient with a primary right lumbar curve and a less pronounced left thoracic curve. In this case, the left rope would be attached towards the top of the vest and the right rope close to the bottom. Patients were instructed to synchronize their breathing with the pull of the ropes and to maintain a straight posture throughout the therapy in order to exercise the musculature on the concave sides of their spinal curves.

Throughout the experiment, the therapist monitored each patient's posture and offered guidance as needed to ensure that the exercises were performed correctly. A measurement of each individual's symptoms was obtained using a scoliometer before the first session and after the entire set. At the end of each set of sessions a questionnaire (see next section) was answered by the therapist and the respective patient. Furthermore, both were encouraged to express any additional comments regarding their user experience.

Results Table 1 contains the measurements that were obtained concerning the severity of each patient's scoliosis. Complementing that, table 2 summarizes the results of the questionnaire. For a full matrix revealing each individual datum, please refer to the accompanying material.

4.3. Discussion

We will begin the discussion of the proposed system by focusing on the results of the user study. All participants stated that they would like to try a similar type of therapy again. Eight out of nine found the treatment enjoyable. This indicates that, should the medical effectiveness of the approach be verified in clinical trials, VR-based hippotherapy could constitute a valuable tool for the conservative treatment of idiopathic scoliosis.

Two participants gave no definitive answer when asked which visualization mode they preferred. Upon further inquiry, both stated that they like to keep their eyes closed during scoliosis exercises in order to concentrate. A future version of the system could incorporate auditory stimuli to support that use case. Out of the remaining seven patients, only one preferred the screen mode, elaborating that they perceived the HMD as unnecessary. We therefore surmise that both modes have their applications and should be considered in further research. However, the majority of participants favored the

HMD which reinforces the notion that full sensory immersion is desirable in the context of virtual hippotherapy.

Two patients reported feelings of discomfort after finishing their final therapy session. Interestingly, these were the same participants who stated that they used the simulator with their eyes closed. In light of research which suggests that the presence of a horizon line can reduce motion sickness [TGW*12, HKH20], this casts some doubt on the usability of our system without visual stimuli. If such cases present themselves in further investigations, the aforementioned option of stopping the saddle altogether, while not utilized by the therapist in this test series, could prove useful. Out of the remaining patients, none reported vertigo or discomfort, indicating that our integration of physical movements with visually induced motion perception was successful. However, we acknowledge that our analysis covers only a subset of the factors commonly associated with simulator sickness. A subsequent quantitative study would benefit from the inclusion of a more comprehensive measurement such as the Simulator Sickness Questionnaire [KLBL93].

With regards to the medical efficacy of the proposed method, our findings are inconclusive. All participants reported that they were able to perceive distinct forces as applied by the ropes. However, while some exhibited clear improvements (6, 7, 8), changes in others were either minor (3) or bidirectional (1, 2, 4, 5, 9). In order to reach a more reliable assessment, future research needs to examine a greater number of patients over a longer period of time. Furthermore, while the scoliometer is quick and straightforward to apply, it does not afford the precision of more involved measurement techniques such as radiography or 3D scanning. Moreover, we observed several participants instinctively straighten their backs after donning the HMD for the first time. This could indicate that some of the positive effects of conventional hippotherapy carry over into virtual reality. However, more data is required to confirm this assumption.

The therapist who guided our patients through the study judged the experience of working with the prototype favorably, noting that the GUI offers an efficient way of creating a force progression which matches an individual patient's breathing rhythm. Concerning the therapeutic suitability of the haptic feedback system, the therapist identified three cases where the garment was not fitted tightly enough, causing the forces to be applied outside of the desired area. This should be addressed by an improved version of the prototype. In all other cases, the device was perceived as readily adaptable to the type of scoliosis at hand. Overall, the therapist described the system as a promising addition to the practice of physical therapy.

It should also be noted that due to the within-subjects design of the study, carry-over effects between the two visualization modes are to be expected. Future quantitative studies could provide more accurate results by utilizing a between-groups setup. Furthermore, the generated path offers little to no additional information to the participants of the study due to the rhythmic and predictable nature of the treatment regimen chosen by the therapist (see figure 3). Thus, the suitability of our path generation algorithm as a visual aid for anticipating lateral forces remains an open question. Finally, future trials could investigate the usability of the GUI on handheld

Patient	Age	Type	Thoracic A	Thoracic B	Thoracic Δ	Lumbar A	Lumbar B	Lumbar Δ
1	30	4BHR	6.0	4.0	-2.0	0.8	1.7	0.9
2	13	4BHR	3.5	1.7	-1.8	2.5	4.5	2.0
3	32	3BR	2.6	3.0	0.4	1.0	1.0	0.0
4	31	4BHR	2.0	2.9	0.9	1.0	0.3	-0.7
5	14	4BHR	3.0	4.0	1.0	2.0	1.0	-1.0
6	30	3BH	3.0	2.0	-1.0	2.0	1.2	-0.8
7	25	3BHR	1.0	0.0	-1.0	1.0	0.0	-1.0
8	18	3LR	1.7	0.4	-1.3	1.2	0.0	-1.2
9	21	3BHL	0.9	0.5	-0.4	0.0	1.5	1.5

Table 1: Comparison of symptoms before (A) and after (B) the set of therapy sessions as well as the difference (Δ) between both measurements. Scoliosis type is given according to the Schroth classification. Data was obtained using a scoliometer.

Question	Positive	Uncertain	Negative
1) Which display mode did you like more?	6	2	1
2) Did you experience vertigo during or after the therapy?	0	0	9
3) Did you perceive the forces applied by the ropes distinctly?	9	0	0
4) Would you try this kind of therapy again?	9	0	0
5) Did you experience discomfort during or after the therapy?	2	0	7
6) Was the treatment enjoyable?	8	1	0
7) Could the type of scoliosis at hand be adequately treated using the vest and ropes?	6	1	2
8) Did you observe changes in the symptoms of the patient?	8	0	1

Table 2: Results of the questionnaire with the number of positive, uncertain and negative answers to each question. For question 1, positive answers correspond to the VR mode and negative answers to the screen mode. Questions 1 through 6 were directed towards the patient, 7 and 8 towards the therapist.

devices and the impact of the wireless network connection implied by that use case.

On a modern consumer-grade PC, the visualization runs smoothly at the desired frame rate and the preprocessing steps complete in a reasonable amount of time. The proposed synchronization measures produce no noticeable visual artifacts. Nevertheless, a more sophisticated prediction algorithm could reduce the discrepancies described in section 4.1 by taking advantage of the periodic nature of the signal.

5. Conclusion and Future Work

We have presented a prototype of an integrated VR system for use in physical therapy with a specific focus on the conservative treatment of idiopathic scoliosis. Our solution consists of the therapy machine itself, a GUI for use by the therapist and a visualization component. The conducted user study showed that our system has the potential to be integrated into physical therapy sessions with patients suffering from idiopathic scoliosis. Thus, it facilitates future quantitative assessments of the medical efficacy of virtual hippotherapy in this context. Such trials could also investigate some aspects of the prototype which have not been examined as part of our study.

Concerning the prototype itself, several possible improvements remain as topics for further research: A more sophisticated visual presentation as well as the inclusion of auditory stimuli can be expected to increase realism and thereby enhance immersion. Furthermore, the system could be extended to allow direct user input,

for example through VR controllers that represent the horse's reins. Finally, a terrain generator that produces more varied environments without violating the constraints set by the predetermined path may induce a more intriguing user experience and avoid boredom during protracted therapy sessions.

Acknowledgments

This work has been funded by the German Bundesministerium für Wirtschaft und Energie in the context of the Zentrales Innovationsprojekt Mittelstand (Förderkennzeichen ZF4392102DB8). We would also like to extend special thanks to Cornelius Winkler for his expertise in the treatment of idiopathic scoliosis as well as his aid in preparing and supervising the user study.

References

- [AABB10] ANDERSON F., ANNETT M., BISCHOF W. F., BOULANGER P.: Virtual equine assisted therapy. In *2010 IEEE Virtual Reality Conference (VR)* (2010), IEEE, pp. 255–256. 2
- [AGHWK16] ANTHES C., GARCÍA-HERNÁNDEZ R. J., WIEDEMANN M., KRANZLMÜLLER D.: State of the art of virtual reality technology. In *2016 IEEE Aerospace Conference* (2016), IEEE, pp. 1–19. 1, 2
- [AKB*15] ANGOULES A. G., KOUKOULAS D., BALAKATOUNIS K., KAPARI I., MATSOUKI E.: A review of efficacy of hippotherapy for the treatment of musculoskeletal disorders. *Journal of Advances in Medicine and Medical Research* (2015), 289–297. 1, 2
- [AML*16] ALDRIDGE R. L., MORGAN A., LEWIS A., ET AL.: The effects of hippotherapy on motor performance in veterans with disabilities: a case report. *Journal of Military and Veterans Health* 24, 3 (2016), 24. 2

- [BK13] BYEON Y.-H., KWAK K.-C.: Analysis of domestic and international development trend for horse riding simulator. In *2013 13th International Conference on Control, Automation and Systems (ICCAS 2013)* (2013), IEEE, pp. 1258–1260. 2
- [BMG03] BENDA W., MCGIBBON N. H., GRANT K. L.: Improvements in muscle symmetry in children with cerebral palsy after equine-assisted therapy (hippotherapy). *The Journal of Alternative & Complementary Medicine* 9, 6 (2003), 817–825. 2
- [EMP*03] EBERT D. S., MUSGRAVE F. K., PEACHEY D., PERLIN K., HART J. C., WORLEY S.: *Texturing & modeling: a procedural approach*. Morgan Kaufmann, 2003. 4
- [FKC*05] FELLS S., KINOSHITA Y., CHEN T.-P. G., TAKAMA Y., YOHANAN S., GADD A., TAKAHASHI S., FUNAHASHI K.: Swimming across the pacific: a vr swimming interface. *IEEE Computer Graphics and Applications* 25, 1 (2005), 24–31. 2
- [Gre05] GREEN S.: Implementing improved perlin noise. *GPU Gems 2* (2005), 409–416. 4
- [GTC*15] GROMALA D., TONG X., CHOO A., KARAMNEJAD M., SHAW C. D.: The virtual meditative walk: virtual reality therapy for chronic pain management. In *Proceedings of the 33rd Annual ACM Conference on Human Factors in Computing Systems* (2015), pp. 521–524. 2
- [HKH20] HEMMERICH W., KESHAVARZ B., HECHT H.: Visually induced motion sickness on the horizon. *Frontiers in Virtual Reality* 1 (2020), 30. 7
- [HKK*12] HAN J. Y., KIM J. M., KIM S. K., CHUNG J. S., LEE H.-C., LIM J. K., LEE J., PARK K. Y.: Therapeutic effects of mechanical horseback riding on gait and balance ability in stroke patients. *Annals of rehabilitation medicine* 36, 6 (2012), 762. 2
- [HNF*05] HAMMER A., NILSAGÅRD Y., FORSBERG A., PEPA H., SKARGREN E., ÖBERG B.: Evaluation of therapeutic riding (sweden)/hippotherapy (united states). a single-subject experimental design study replicated in eleven patients with multiple sclerosis. *Physiotherapy theory and practice* 21, 1 (2005), 51–77. 2
- [JGS*15] JANURA M., GALLO J., SVOBODA Z., SVIDERNOCHOVÁ D., KRISTINÍKOVÁ J.: Effect of physiotherapy and hippotherapy on kinematics of lower limbs during walking in patients with chronic low back pain: A pilot study. *Journal of Physical Education and Sport* 15, 4 (2015), 663. 2
- [KAE*07] KAMTSIURIS P., ATZPODIEN K., ELLERT U., SCHLACK R., SCHLAUD M.: Prevalence of somatic diseases in german children and adolescents. results of the german health interview and examination survey for children and adolescents (kiggs). *Bundesgesundheitsblatt, Gesundheitsforschung, Gesundheitsschutz* 50, 5-6 (2007), 686–700. 2
- [KJH*18] KARUNANAYAKA K., JOHARI N., HARIRI S., CAMELIA H., BIELAWSKI K. S., CHEOK A. D.: New thermal taste actuation technology for future multisensory virtual reality and internet. *IEEE transactions on visualization and computer graphics* 24, 4 (2018), 1496–1505. 2
- [KLBL93] KENNEDY R. S., LANE N. E., BERBAUM K. S., LILIENTHAL M. G.: Simulator sickness questionnaire: An enhanced method for quantifying simulator sickness. *The international journal of aviation psychology* 3, 3 (1993), 203–220. 7
- [KNS19] KIM H. W., NAM K. S., SON S. M.: Effects of virtual reality horse riding simulator training using a head-mounted display on balance and gait functions in children with cerebral palsy: A preliminary pilot study. *The Journal of Korean Physical Therapy* 31, 5 (2019), 273–278. 2
- [KSK13] KONIECZNY M. R., SENYURT H., KRAUSPE R.: Epidemiology of adolescent idiopathic scoliosis. *Journal of children's orthopaedics* 7, 1 (2013), 3–9. 2
- [LG13] LEVAC D. E., GALVIN J.: When is virtual reality “therapy”? *Archives of physical medicine and rehabilitation* 94, 4 (2013), 795–798. 2
- [LMM12] LEVAC D., MILLER P., MISSIUNA C.: Usual and virtual reality video game-based physiotherapy for children and youth with acquired brain injuries. *Physical & occupational therapy in pediatrics* 32, 2 (2012), 180–195. 2
- [LPYS04] LINDEMAN R. W., PAGE R., YANAGIDA Y., SIBERT J. L.: Towards full-body haptic feedback: the design and deployment of a spatialized vibrotactile feedback system. In *Proceedings of the ACM symposium on Virtual reality software and technology* (2004), pp. 146–149. 2
- [LS92] LEHNERT-SCHROTH C.: Introduction to the three-dimensional scoliosis treatment according to schroth. *Physiotherapy* 78, 11 (1992), 810–815. 2
- [MBDSS09] MCGIBBON N. H., BENDA W., DUNCAN B. R., SILKWOOD-SHERER D.: Immediate and long-term effects of hippotherapy on symmetry of adductor muscle activity and functional ability in children with spastic cerebral palsy. *Archives of physical medicine and rehabilitation* 90, 6 (2009), 966–974. 2
- [MNI11] MATSUKURA H., NIHEI T., ISHIDA H.: Multi-sensorial field display: Presenting spatial distribution of airflow and odor. In *2011 IEEE Virtual Reality Conference* (2011), IEEE, pp. 119–122. 2
- [NB16] NABIYOUNI M., BOWMAN D. A.: A taxonomy for designing walking-based locomotion techniques for virtual reality. In *Proceedings of the 2016 ACM Companion on Interactive Surfaces and Spaces*. 2016, pp. 115–121. 2
- [PCSB*18] PADILLA-CASTAÑEDA M. A., SOTGIU E., BARSOTTI M., FRISOLI A., ORSINI P., MARTIRADONNA A., LADDAGA C., BERGAMASCO M.: An orthopaedic robotic-assisted rehabilitation method of the forearm in virtual reality physiotherapy. *Journal of healthcare engineering* 2018 (2018). 2
- [Per85] PERLIN K.: An image synthesizer. *ACM Siggraph Computer Graphics* 19, 3 (1985), 287–296. 4
- [Per02] PERLIN K.: Improving noise. In *Proceedings of the 29th annual conference on Computer graphics and interactive techniques* (2002), pp. 681–682. 4
- [RLZ21] REN C., LIU T., ZHANG J.: Horse-riding simulators in treatment of chronic low back pain: A meta-analysis. *International Journal of Clinical Practice* (2021), e14198. 2
- [Sho85] SHOEMAKE K.: Animating rotation with quaternion curves. In *Proceedings of the 12th annual conference on Computer graphics and interactive techniques* (1985), pp. 245–254. 5
- [TGW*12] TAL D., GONEN A., WIENER G., BAR R., GIL A., NACHUM Z., SHUPAK A.: Artificial horizon effects on motion sickness and performance. *Otology & Neurotology* 33, 5 (2012), 878–885. 7
- [WGN*16] WIBMER C., GROEBL P., NISCHELWITZER A., SALCHINGER B., SPERL M., WEGMANN H., HOLZER H.-P., SARAPH V.: Video-game-assisted physiotherapeutic scoliosis-specific exercises for idiopathic scoliosis: case series and introduction of a new tool to increase motivation and precision of exercise performance. *Scoliosis and spinal disorders* 11, 1 (2016), 1–9. 2
- [WKL14] WEISS P. L., KESHNER E. A., LEVIN M. F.: *Virtual reality for physical and motor rehabilitation*. Springer, 2014. 1, 2
- [WW05] WIEDERHOLD B. K., WIEDERHOLD M. D.: *Virtual reality therapy for anxiety disorders: Advances in evaluation and treatment*. American Psychological Association, 2005. 2
- [YÇD*17] YELVAR G. D. Y., ÇIRAK Y., DALKILINÇ M., DEMIR Y. P., GUNER Z., BOYDAK A.: Is physiotherapy integrated virtual walking effective on pain, function, and kinesiophobia in patients with non-specific low-back pain? randomised controlled trial. *European Spine Journal* 26, 2 (2017), 538–545. 2